Rev.Adv.Mater.Sci. 21(2009) 99-105

# AMORPHOUS INTERGRANULAR BOUNDARIES AS TOUGHENING ELEMENTS IN NANOCRYSTALLINE CERAMICS

**S.V. Bobylev[1], A.K. Mukherjee[2], I.A. Ovid'ko[1] and A.G. Sheinerman[1]**

[1]Institute of Problems of Mechanical Engineering, Russian Academy of Sciences, Bolshoj 61, Vasil. Ostrov, St. Petersburg 199178, Russia
[2]Department of Chemical Engineering and Materials Science, University of California, Davis, 1 Shields Avenue, Davis, CA 95616, USA

*Received: April 12, 2009*

**Abstract.** A theoretical model is suggested that describes the role of amorphous intergranular boundaries as toughening elements in deformed nanocrystalline ceramics. Within the model, immobile lattice dislocations are generated at amorphous intergranular boundaries (through local shear events) under external stress concentrated near crack tips. The dislocations cause a partial stress relaxation in vicinities of crack tips and thereby enhance fracture toughness. It is shown that the dislocation generation is energetically favorable and effective in toughness enhancement in nanocrystalline SiC with amorphous intergranular boundaries.

## 1. INTRODUCTION

Nanocrystalline ceramics (nc-ceramics) show the outstanding mechanical properties such as superstrength, superhardness and good wear resistance in wide temperature ranges [1–14]. However, in most cases, nc-ceramics exhibit low fracture toughness which considerably limits their practical utility; see, e.g., review [1]. At the same time, several research groups reported on toughness enhancement of nc-ceramics, compared to that of their microcrystalline counterparts [1–6]. (Also, there are situations where nanocrystalline composites show enhanced toughness characteristics due to other factors associated with the presence of second-phase nanoparticles or carbon nanotubes [1,7–9].) With these examples and the specific structural features of nc-ceramics, one expects that there are toughening mechanisms that effectively operate in nc-ceramics but are not effective in microcrystalline ceramics. In this context, from both fundamental and applied viewpoints, there is a large interest in understanding the toughening mechanisms specific for nc-ceramics. Recently, several toughening mechanisms – nanoscale deformation twinning [15], activity of lattice dislocations emitted from nanoparticles [16] and stress-driven migration of grain boundaries [17] – have been suggested as those specific for nc-ceramics. Besides, we think that intergrain sliding can significantly contribute to toughening of nc-ceramics, where intergranular boundaries often have the amorphous structure and occupy very large volume fractions. This view is based on the fact that the deformation behavior of nc-ceramics is strongly influenced by amorphous intergranular boundaries (AIBs); see, e.g., experimental data [2,10–12] and computer simulations [18,19]. For instance, following computer simulations [18,19] of evolution of the nanocrystalline cubic phase of silicon carbide (3C-SiC) under a mechanical load, plastic deformation intensively occurs within AIBs in these nc-ceramics. In the con-

Corresponding author: I. A. Ovid'ko, e-mail: ovidko@def.ipme.ru

text discussed, it is natural to think that AIBs can effectively serve as toughening structural elements in nanocrystalline ceramic specimens with cracks. The main aim of this paper is to suggest a theoretical model describing the hampering effects of AIBs on crack growth and corresponding enhancement of fracture toughness in nc-ceramics.

## 2. GENERATION OF DISLOCATIONS DUE TO INTERGRAIN SLIDING ALONG AMORPHOUS INTERGRANULAR BOUNDARIES IN NANOCRYSTALLINE CERAMICS

Let us consider a nc-ceramic solid consisting of nanoscale grains divided by AIBs. A two-dimensional section of a typical fragment of the solid containing a long flat crack of length $l$ is schematically shown in Fig. 1. The crack intersects the central AIB at the point distant by $r$ ($r << l$) from the nearest triple junction of AIBs (Fig. 1). In the coordinate system shown in Fig. 1b, the crack is located along the coordinate axis $x$ in the region $x<0$. For simplicity, we assume that the defect structure of the solid is the same along the coordinate axis $z$ perpendicular to the $xy$ plane shown in Fig. 1b. This assumption will allow us to simplify a mathematical analysis of the problem, reducing it to consideration of a two-dimensional structure and its evolution under mechanical load. At the same time, the two-dimensional description definitely reflects the key aspects of the problem under our study. In the two-dimensional picture (Fig. 1b), the crack line is perpendicular to the direction of the external tensile stress $\sigma_0$ action. That is, the crack is a mode I crack. Also, within our model, the ceramic specimen is assumed to be elastically isotropic solid having the shear modulus $\mu$ and the Poisson ratio $\nu$.

High level stresses operating in deformed nanoceramics, with stress concentration near crack tips taken into account, can initiate intergrain sliding along AIBs near crack tips (Fig. 1b). Such processes of intergrain sliding along AIBs in nanoceramics are capable of producing edge dislocations at triple junctions bounding the AIBs [20]. In this paper, we consider the situation where intergrain sliding occurs in a part of the AIB, located between the crack tip and a triple junction, and results in the formation of an edge dislocation located at the triple junction nearest to the crack tip, as shown in Fig. 1b. The dislocation creates stresses that influence crack growth.

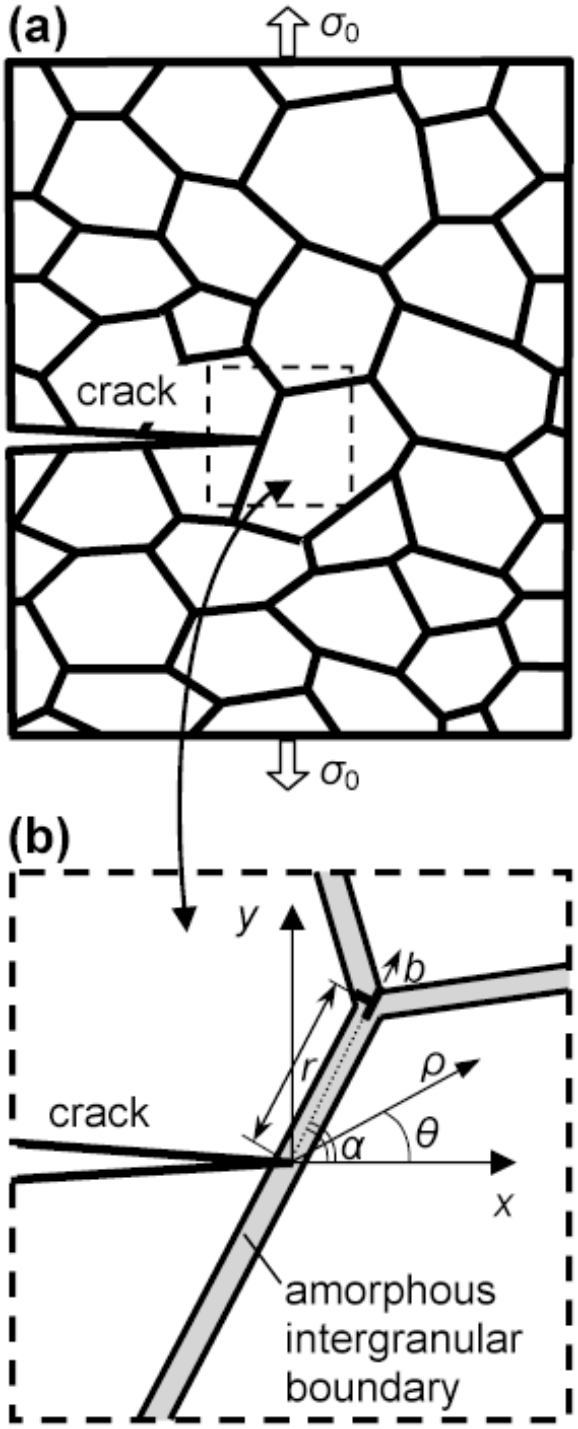


**Fig. 1.** Long crack in a nanocrystalline ceramic specimen being under external tensile load $\sigma_0$. (a) General view. (b) The magnified inset highlights generation of edge dislocation at amorphous intergranular boundary near tip of long crack that intersects the boundary.

Note that the effects of conventional lattice dislocations on crack growth were previously studied

by several researchers; see, e.g., [21–23]. However, the case under our consideration has its specific features. First of all, the crack-stimulated generation of dislocations occurs at AIBs (but not in grain interiors) intersected by cracks (Fig. 1b). This process is expected to be specific precisely for nc-ceramics, because they are specified by very large volume fractions occupied by both AIBs and their triple junctions. Events of intersection of a growing crack and AIBs in conventional microcrystalline ceramics are rare, in which case one can neglect their effects on crack growth. Second, the dislocations (Fig. 1b) result from intergrain sliding along AIBs. In this case, the Burgers vector magnitude of each dislocation at an AIB gradually grows (due to occurrence of local shear events, carriers of intergrain sliding in AIBs) in parallel with local plastic strain carried by intergrain sliding in this AIB; for details, see [20]. Such dislocations are treated in terms of the Volterra theory of dislocations in continuum media [24,25] as dislocation-like sources of internal stresses (but not conventional lattice dislocations). In doing so, such dislocations are commonly immobile at triple junctions of AIBs (Fig. 1b).

To summarize, crack-stimulated intergrain sliding along an AIB produces an immobile dislocation near the crack tip (Fig. 1). The direction of the dislocation Burgers vector is parallel with the AIB line (plane in the three-dimensional case), while its magnitude is arbitrary and gradually grows in parallel with local plastic strain carried by intergrain sliding within the AIB.

## 3. EFFECTS OF DISLOCATIONS PRODUCED BY INTERGRAIN SLIDING ALONG AMORPHOUS INTERGRANULAR BOUNDARIES ON FRACTURE TOUGHNESS OF NANOCRYSTALLINE CERAMICS

Let us consider the effect of intergrain-sliding-produced dislocation at the AIB (Fig. 1) on fracture toughness of a nanoceramic solid. To do so, we will use the standard crack growth criterion [26] based on the balance between the driving force related to a decrease in the elastic energy and the hampering force related to occurrence of a new free surface during crack growth. This criterion is given as [26]:

$$\frac{1-\nu}{2\mu}\left(K_I^2 + K_{II}^2\right) = 2\gamma, \tag{1}$$

where $K_I$ and $K_{II}$ are the intensity factors for normal (to crack line in the two-dimensional case) and shear stresses, respectively; and $\gamma$ is the specific energy of the free surface occurring due to crack growth. In the considered situation where the crack growth direction is perpendicular to the external load direction, the coefficients $K_I$ and $K_{II}$ are given as:

$$\begin{aligned} K_I &= K_I^{\sigma} + k_I^d, \\ K_{II} &= k_{II}^d. \end{aligned} \tag{2}$$

Here $K_I^{\sigma}$ is the intensity factor for the external stress $\sigma_0$, while $k_I^d$ and $k_{II}^d$ are the intensity factors for the stresses created by the edge dislocation located near the crack tip (Fig. 1).

Within the macroscopic mechanical description, the effect of the local plastic flow (intergrain sliding resulting in the formation of a dislocation) on crack growth can be accounted for through the introduction of the effective fracture toughness $K_{IC}$. In this case, the crack is considered as that propagating under the action of the tensile load perpendicular to the crack growth direction, while the presence of the dislocation just changes the value of $K_{IC}$ compared to the case of brittle crack propagation. In these circumstances, the critical condition for the crack growth can be represented as (see, e.g., Ref. [27]): $K_I^{\sigma} = K_{IC}$.

With the expressions (2) substituted to formula (1), and the critical condition $K_I^{\sigma} = K_{IC}$ taken into account, one finds the following expression for the factor $K_{IC}$:

$$K_{IC} = \sqrt{\frac{4\mu\gamma}{1-\nu} - \left(k_{II}^d\right)^2} - k_I^d. \tag{3}$$

In order to characterize the effect of dislocations produced by intergrain sliding (Fig. 1) on crack growth, one should compare the value $K_{IC}$ with the fracture toughness $K_{IC}^0 = \sqrt{4\mu\gamma / (1-\nu)}$ in the dislocation-free case, that is, the case of brittle fracture with the intergrain sliding being completely suppressed.

Let us calculate the effective fracture toughness $K_{IC}$ in the situation where the dislocation is located near the crack, as shown in Fig. 1b. In doing so, $b$ denotes the Burgers vector magnitude of the dislocation, $r$ the distance between the dislocation and the crack tip, $\alpha$ the angle made by the AIB plane (or the dislocation Burgers vector) and the coordinate axis O$x$. The stress intensity factors $k_i^d$ and $k_{Ii}^d$ for the dislocation-induced stresses are calcu-

lated in [21,22]. With the results of these papers, we have:

$$k_I^d = -\frac{3\pi Db\sin\alpha\cos(\alpha/2)}{\sqrt{2\pi r}},$$
$$k_{II}^d = -\frac{\pi Db\left[\cos(\alpha/2)+3\cos(3\alpha/2)\right]}{2\sqrt{2\pi r}}, \quad (4)$$

where $D = \mu/[2\pi(1-\nu)]$.

In our model, the Burgers vector magnitude $b$, figuring in formulas (4), is arbitrary, because the magnitude $b$ is equal to the jump of displacements produced by the intergrain sliding in the boundary plane; for details, see [20]. In the quasi-equilibrium state, the Burgers vector magnitude $b$ corresponds to minimum of the energy change $\Delta W$ associated with the dislocation generation process (Fig. 1b). In the situation under consideration, the energy change $\Delta W$ has three terms:

$$\Delta W = W_s + W_c - A. \quad (5)$$

Here $W_s$ is the proper elastic energy of the dislocation; $W_c$ is the dislocation core energy, and $A$ denotes the work of the shear stress, spent to generation of the dislocation.

Since the dislocation (Fig. 1b) is located near the crack free surface, its stresses are screened. The proper energy of such a dislocation is calculated with the aid of formula [21] taking into account the image forces that characterize the screening effect. In doing so, we have:

$$W_s \approx \frac{Db^2}{2}\ln\frac{r}{r_c}. \quad (6)$$

Here $r_c$ is the dislocation core radius. The dislocation core energy $W_c$ in the standard approximation is given as [25]: $W_c \approx Db^2/2$

The work $A$ of the shear stress, spent to generation of the dislocation, is calculated in the standard way [28] as the work spent to movement of the dislocation from the crack tip to its final position (shown in Fig. 1b). At the same time, in the case under our study, one should take into account the fact that the dislocation is generated through local shear events occurring in the amorphous intergranular phase. In doing so, we should take into consideration the additional term characterizing the resistance of the amorphous phase to plastic shear (local shear events) resulting in the formation of the dislocation. Following [20,29], in a first approximation, we assume that the resistance of the amorphous phase to plastic shear is described as the friction force which acts on the moving dislocation and is equal by magnitude to $b\tau_a$, where $\tau_a$ is the flow stress for the amorphous intergranular phase. According to this assumption, plastic shear in the AIB occurs, if the local shear stresses $\geq\tau_a$ at every point of the AIB. Then, the work $A$ is represented in the following form:

$$A = b\int_0^r \sigma_{r\theta}(\rho,\theta=\alpha)\,d\rho - \tau_a br,$$
$$\sigma_{r\theta}(r,\theta=\alpha) \geq \tau_a. \quad (7)$$

Here $\sigma_{r\theta}(\rho,\theta)$ is the stress tensor component (written in the polar coordinate system $(\rho,\theta)$ having its center at the crack tip; see Fig. 1) created by the constant external one-axis tensile load in the vicinity of the crack tip. The inequality $\sigma_{r\theta}(\rho,\theta=\alpha) \geq \tau_a$ gives the necessary condition for intergrain sliding in the plane making the angle a with the coordinate axis O$x$, in the interval $0 < \rho < r$. The expression for the stress $\sigma_{r\theta}(\rho,\theta)$ is given as (see, e.g., Ref. [27]):

$$\sigma_{r\theta}(\rho,\theta) = \frac{K_I^\sigma \sin\theta\cos(\theta/2)}{2\sqrt{2\pi\rho}}. \quad (8)$$

After substitution of formula (8) to formula (7) and subsequent integration, one finds:

$$A = br\left(\frac{K_I^\sigma \sin\alpha\cos(\alpha/2)}{\sqrt{2\pi r}} - \tau_\alpha\right),$$
$$K_I^\sigma \geq \frac{\tau_a\sqrt{8\pi r}}{\sin\alpha\cos(\alpha/2)}. \quad (9)$$

Then, with formulas (6) and (9) as well as the expression for $W_c$, we obtain the following formula for the characteristic energy change $\Delta W$:

$$\Delta W = \frac{Db^2}{2}\left(\ln\frac{r}{r_c}+1\right)$$
$$-br\left(\frac{K_I^\sigma \sin\alpha\cos(\alpha/2)}{\sqrt{2\pi r}} - \tau_a\right),$$
$$K_I^\sigma \geq \frac{\tau_a\sqrt{8\pi r}}{\sin\alpha\cos(\alpha/2)}. \quad (10)$$

From the condition $\partial(\Delta W)/\partial b = 0$ of the minimum of the energy change $\Delta W$ one finds the following expression for the Burgers vector magnitude $b$ of the dislocation:

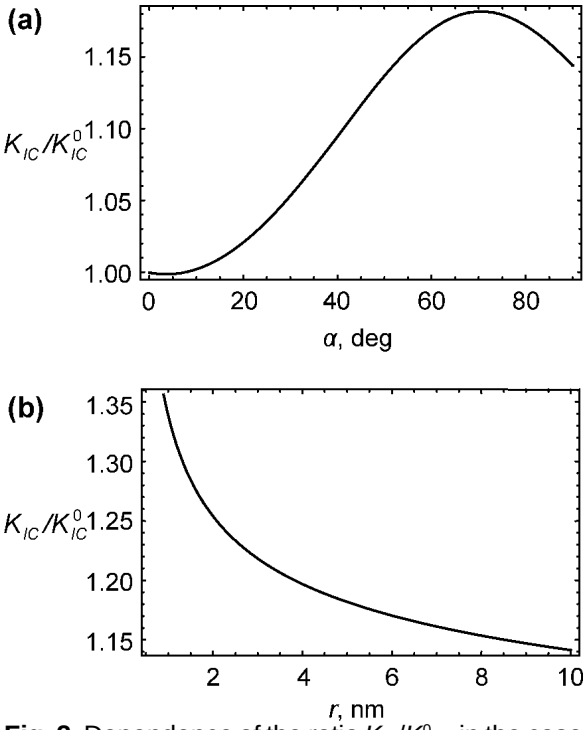


**Fig. 2.** Dependence of the ratio $K_{IC}/K^0_{IC}$, in the case of edge dislocation located near crack tip, on (a) angle α made by the Burgers vector (or amorphous boundary plane) with crack growth direction, for $r$ = 5 nm; and (b) on distance $r$ between the crack tip and the dislocation, for α = 70°.

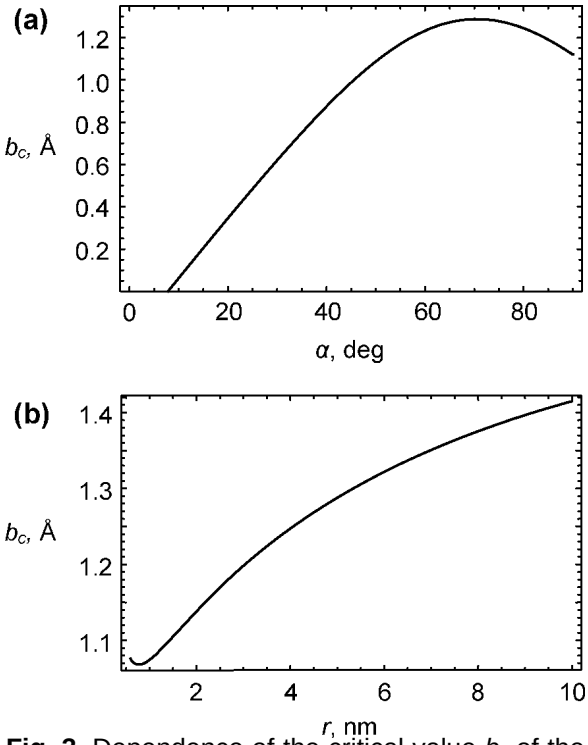


**Fig. 3.** Dependence of the critical value $b_c$ of the Burgers vector of the dislocation located near crack tip (for details, see text) on (a) angle α made by the Burgers vector (or amorphous boundary plane) with crack growth direction, for $r$ = 5 nm; and (b) on distance $r$ between the crack tip and the dislocation, for α = 70°.

$$b = \frac{(1-\nu)\sqrt{2\pi r}}{\mu\left[\ln(r/r_c)+1\right]} \times \left(K_I^{\sigma}\sin\alpha\cos(\alpha/2) - \tau_a\sqrt{2\pi r}\right), \qquad K_I^{\sigma} \geq \frac{\tau_a\sqrt{8\pi r}}{\sin\alpha\cos(\alpha/2)}. \tag{11}$$

With formulas (4) and (11), we express the intensity factors $k_I^d$ and $k_{II}^d$ of the dislocation-induced stresses through $K_I^{\sigma}$. After substitution of formulas (4) and (11) as well as the equation $K_I^{\sigma} = K_{IC}$ into formula (3), we obtain the following equation for the critical value of the stress intensity factor $K_{IC}$:

$$PK_{IC}^2 + QK_{IC} + R = 0, \tag{12}$$

where

$$P = 8\left(\ln(r/r_c)+1\right)^2 - \sin^2\alpha\cos^2(\alpha/2)\times\left[24\ln(r/r_c) + 3\cos 2\alpha - 4\cos\alpha + 17\right], \tag{13}$$

$$Q = 2\tau_a\sqrt{2\pi r}\sin\alpha\cos^2(\alpha/2)\times\left[12\ln(r/r_c) + 3\cos 2\alpha - 4\cos\alpha + 5\right], \tag{14}$$

$$R = 8\pi r\tau_a^2\cos^2(\alpha/2)\left[5 - 3\cos\alpha\right] - 64\pi D\gamma\left(\ln(r/r_c)+1\right)^2. \tag{15}$$

Analysis of Eq. (12) shows that the equation always has a positive solution given as:

$$K_{IC} = \frac{-Q + \sqrt{Q^2 - 4PR}}{2P}. \tag{16}$$

Let us calculate the effective fracture toughness $K_{IC}$ in the exemplary case of nanocrystalline ceramic 3C-SiC (the cubic phase of silicon carbide). In doing so, for 3C-SiC, we will use the following typical values of parameters: μ = 217 GPa, ν = 0.23 [30] and γ = 1.5 J/m² [31]. The dislocation core radius is taken as $r_c \approx 0.1$ nm. This value is approxi-

mately equal to typical values of the Burgers vector magnitude of the dislocation, resulting from our calculations (see below).

With formulas (13)–(16), the effective fracture toughness $K_{IC}$ depends on the flow stress $\tau_a$ of the amorphous phase. In general, $\tau_a$ is highly sensitive to both temperature and strain rate. For low temperatures and/or high strain rates, athermal plastic deformation occurs. Following experiments [32], the microhardness $H_V$ of amorphous SiC is around 30 GPa. This value of $H_V$, according to the standard relation $\tau_f \approx H_V/6$ between $H_V$ and athermal flow stress $\tau_f$ [33], corresponds to the athermal flow stress $\tau_a$=5 GPa of amorphous SiC. The stress level significantly decreases with rising temperature and/or decreasing strain rate, in which case thermally-assisted deformation occurs. In our following consideration concerning thermally-assisted deformation, for definiteness, we will take $\tau_a$ = 1 GPa.

The dependence of the ratio $K_{IC}/K^0_{IC}$ on the angle $\alpha$, for $r$ = 5 nm, is presented in Fig. 2a. From this figure it follows that the local fracture toughness $K_{IC}$ reaches its maximum value when the AIB plane (and thereby the Burgers vector of the dislocation) makes the angle of around 70° with the direction of crack growth. This is related to the fact that the stress $\alpha_{r\theta}(\rho,\alpha)$ is maximum when the plane makes the angle ≈ 70° with the direction of crack growth. The dependence of $K_{IC}$ on the distance $r$ between the dislocation and the crack tip, for $\alpha$ = 70°, is presented in Fig. 2b. From this figure it follows that the dislocation formation leads to increase of $K_{IC}$ by ≈ 30%, when $r \approx 1$ nm. This effect is significant, but the increase in $K_{IC}$ rapidly falls with increasing $r$.

In order to characterize the fracture toughness, one can use stresses and crack length, instead of stress intensity factors. The crack length $l$ is in the following relationship with the stress intensity factor (see, e.g., [27]): $K_I^{\sigma} = \sigma_0\sqrt{\pi l/2}$. The results of our previous calculations can be directly re-formulated in terms of stresses and crack length in the examined situation where the crack length $l$ is large enough ($l >> r$). To do so, we suppose $l$ = 100 nm. For $l$ = 100 nm, the critical stress $\sigma_c^0$ needed to cause the crack growth in the dislocation-free case (the critical stress for brittle fracture) is given as: $\sigma_c^0 = \sqrt{8\mu\gamma/(1-\nu)\pi l} \approx 3.3$ GPa. The dislocation formation (Fig. 1b) leads to increase of the critical stress $\sigma_c$ by value of 15–30% (Fig. 2). For instance, for $\alpha$ = 70°, $\sigma_c \approx 4.1$ GPa at $r$ = 2 nm; $\sigma_c \approx 3.9$ GPa at $r$=5 nm; and $\sigma_c \approx 3.8$ GPa at $r$ = 10 nm.

Fig. 3 shows both the dependences of the Burgers vector magnitude $b$ on the angle $\alpha$ at $r$ = 5 nm (see Fig. 3a) and the dependences of $b$ on the distance $r$ at $\alpha$ = 70° (see Fig. 3b). The dependences presented in Fig. 3 are calculated using formula (11) in the case of $K_I^{\sigma} = K_{IC}$. That is, these dependences show the critical magnitude $b_c(r)$ of the Burgers vector of the dislocation whose formation needs the stress equal to the critical stress for growth of the crack having the dislocation in its vicinity. As a corollary, the dislocation Burgers vector magnitude $b_c$ is the maximum magnitude at given values of $r$ and a, because generation of the dislocation in this point $(r,\alpha)$ with the Burgers vector magnitude $b > b_c$ needs the stress level exceeding the critical stress for crack growth. As it follows from Fig. 3, the typical values of the critical Burgers vector magnitude are around 0.1 nm.

Also, Fig. 3a shows that at $r$ = 5 nm, the dislocation generation is energetically unfavorable in the range of low angles $\alpha < 8°$. The reason is that, for such small angles, the shear stresses $\sigma_{r\theta}(\rho,\theta = \alpha)$ created in the AIB plane by the applied tensile load are small, so that the necessary condition $\sigma_{r\theta}(r = 5$ nm, $\theta = \alpha) \geq \tau_a$ for intergrain sliding in the interval $0 < \rho < r$ is not satisfied.

## 4. CONCLUDING REMARKS

Thus, in this paper, we suggested a theoretical model describing generation of a dislocation at an AIB near the tip of a crack that intersects the boundary (Fig. 1). In the framework of the model, the dislocation represents a dislocation-like source of internal stresses that terminates unfinished plastic shear within the AIB. That is, the dislocation is defined as a non-crystallographic Volterra dislocation (but not as a perfect lattice dislocation in a crystalline lattice). In this situation, the dislocation Burgers vector magnitude is arbitrary and gradually grows in parallel with local plastic strain carried by intergrain sliding within the AIB. (Also, the notion of such non-crystallographic dislocations with continuously growing Burgers vector magnitudes has recently been used in a description of plastic deformation of Gum Metal [34] and homogeneous generation of dislocations in nanocrystalline materials [35].)

In the exemplary case of nanocrystalline ceramic 3C-SiC, we calculated the equilibrium value of Burgers vector magnitude (characterizing plastic shear) for the dislocation under the action of an external tensile stress $\sigma_0$. The typical values of the Burgers vector magnitude are around 0.1 nm. From the force criterion for crack growth, we found that the effective fracture toughness $K_{IC}$ increases by

value of ~30% due to the dislocation generation, when the distance between the dislocation and the crack $r$~1 nm. This effect is significant, but the increase in $K_{IC}$ rapidly falls with increasing $r$. Also, it has been shown that the critical stress for crack growth increases by 15–30% (compared to the dislocation-free case), when the crack intersects the amorphous intergranular boundary at the point distant by 1–10 nm from the nearest triple junction where a dislocation is generated.

The likehood to have a triple junction closely located to a crack tip increases with decreasing the grain size in a nanocrystalline specimen. In these circumstances, the hampering effect of AIBs on crack growth enhances with decreasing the grain size and is essential only in nc-ceramics. In general, both the small grain size and the very high level of stresses operating in nc-ceramics cause the crack-stimulated intergrain sliding along AIBs (Fig. 1) to be the toughening mechanism specific precisely for nc-ceramics and hardly effective in conventional microcrystalline ceramics.

The work was supported, in part, by the National Science Foundation Grant CMMI #0700272, the Office of Naval Research (grant N00014-08-1-0405), the Russian Foundation of Basic Research (Grant 08-01-00225-a), the Russian Academy of Sciences Program “Fundamental problems in mechanics of interactions in technical and natural systems, materials and media”, and the Federal Agency of Science and Innovations (grant MK-1702.2008.1).

## REFERENCES

[1] G.-D. Zhan, J.D. Kuntz and A.K. Mukherjee // *MRS Bull.* **29** (2004) 22.

[2] C.C. Koch, I.A. Ovid’ko, S. Seal and S. Veprek, *Structural Nanocrystalline Materials: Fundamentals and Applications* (Cambridge University Press, Cambridge, 2007).

[3] S. Bhaduri and S.B. Bhaduri // *Nanostruct. Mater.* **8** (1997) 755.

[4] A.A. Kaminskii, M.Sh. Akchurin, R.V. Gainutdinov, K. Takaichi, A. Shirakava, H. Yagi, T. Yanagitani and K. Ueda // *Crystallography Reports* **50** (2005) 869.

[5] Y. Zhao, J. Qian, L.L. Daemen, C. Pantea, J. Zhang, G.A. Voronin and T.W. Zerda // *Appl. Phys. Lett.* **84** (2004) 1356.

[6] Y.T. Pei, D. Galvan D and J.T.M. De Hosson // *Acta Mater.* **53** (2005) 4505.

[7] R.W. Siegel, S.K. Chang, B.J. Ash, J. Stone, P.M. Ajayan, R.W. Doremus and L.S. Schadler // *Scr. Mater.* **44** (2001) 2061.

[8] G.-D. Zhan, J.D. Kuntz, J. Wan and A.K. Mukherjee // *Nature Mater.* **2** (2003) 38.

[9] H. Liu, C. Huang, X. Teng and H.Wang // *Mater. Sci. Eng. A* **487** (2008) 258.

[10] X. Xu, T. Nishimura, N. Hirosaki, R.-J. Xie, T. Yamamoto and H. Tanaka // *Acta Mater*. **54** (2006) 255.

[11] A. Dominguez-Rodriguez, D. Gomez-Garcia, E. Zapata-Solvez, J.Z. Chen and R. Chaim // *Scr. Mater.* **56** (2007) 89.

[12] D.M. Hulbert, D. Jiang, J.D. Kuntz, Y. Kodera and A.K. Mukherjee // *Scr. Mater.* **56** (2007) 1103.

[13] I.A. Ovid’ko and A.G. Sheinerman // *Rev. Adv. Mater. Sci.* **16** (2007) 1.

[14] A. Swiderska-Sroda, G. Kalisz, B. Palosz and N. Herlin-Boime // *Rev. Adv. Mater. Sci.* **18** (2008) 422.

[15] M.Yu. Gutkin, I.A. Ovid’ko and N.V. Skiba // *Philos. Mag.* **88** (2008) 1137.

[16] S.-M. Choi and H. Awaji // *Sci. Tech. Adv. Mater.* **6** (2005) 2.

[17] I.A. Ovid’ko, A.G. Sheinerman and E.C. Aifantis // *Acta Mater*. **56** (2008) 2718.

[18] I. Szlufarska, A. Nakano and P. Vashista // *Science* **309** (2005) 911.

[19] Y. Mo and I. Szlufarska // *Appl. Phys. Lett.* **90** (2007) 181926.

[20] S.V. Bobylev, A.K. Mukherjee and I.A. Ovid’ko // *Scr. Mater.* **60** (2009) 36.

[21] I.-H. Lin and R. Thomson // *Acta Metall.* **34** (1986) 187.

[22] T.-Y. Zhang and J.C.M. Li // *Acta Metall. Mater.* **39** (1991) 2739.

[23] T.-Y. Zhang and J.C.M. Li // *J. Appl. Phys.* **72** (1992) 2215.

[24] V. Volterra // *Ann. Ecole Normale Sup. Paris* **24** (1907) 401.

[25] J.P. Hirth and J. Lothe, *Theory of Dislocations* (Wiley, New York, 1982).

[26] R.G. Irwin // *J. Appl. Mech.* **24** (1957) 361.

[27] *Fracture Mechanics and Strength of Materials*, ed. by V.V. Panasyuk (Naukova Dumka, Kiev, 1988), Vol. 2. (in Russian).

[28] T. Mura, In: *Advances in Materials Research*, ed. by H. Herman (Interscience, New York, 1968), Vol. 3, p. 1.

[29] S.V. Bobylev, M.Yu. Gutkin and I.A. Ovid’ko // *Phys. Sol. State* **50** (2008) 1888.

[30] Z. Ding, S. Zhou and Y. Zhao // *Phys. Rev. B* **70** (2004) 184117.
[31] S.P. Mehandru and A.B. Anderson // *Phys. Rev. B* **42** (1990) 9040.
[32] M.A.E. Khakani, M. Chaker, A. Jean, S. Boily, J.C. Kieffer, M.E. O'Hern, M.F. Ravet and F. Rousseaux // *J. Mater. Res.* **9** (1994) 96.
[33] S. Veprek, A.K. Mukherjee, P. Karvankova, H.-D. Mannling, J.L. He, K. Moto, J. Prochazka and A.S. Argon // *J. Vac. Sci. Technol. A* **21** (2003) 532.
[34] M.Yu. Gutkin, T. Ishizaki, S. Kuramoto and I.A. Ovid'ko // *Acta Mater*. **54** (2006) 2489.
[35] M.Yu. Gutkin and I.A. Ovid'ko // *Acta Mater.* **56** (2008) 1642.